Int. J. Solids Structures, 1971, Vol. 7, pp. 543 to 558. Pergamon Press. Printed in Great Britain

DYNAMIC CONTACT STRESSES PRODUCED BY THE IMPACT OF AN AXISYMMETRICAL PROJECTILE ON AN ELASTIC HALF-SPACE

Y. M. TSAI

Department of Engineering Mechanics and Engineering Research Institute,
Iowa State University, Ames, Iowa

Abstract—The dynamic contact stresses between an axisymmetric projectile and an elastic half-space are obtained by solving three-dimensional equations of motion. These stresses are written as the sums of the Hertz contact stresses and wave-effect integrals. In terms of the contact radius, the Hertz theory is shown to be a good approximation in determining total applied force. However, for calculating the maximum radial surface stress at the maximum contact radius, the Hertz theory applies only when the contact time is longer than approximately 40 μsec. The discrepancy between the Hertz radial stress and the corresponding value obtained here is greater at the initial stage of impact than at the middle of the contact time.

1. INTRODUCTION

WHEN a solid body impinges on the smooth surface of a material, both the size of the contact region and the values of the stresses around the region vary with respect to time. Trying to account for the moving boundary conditions and the inertial effect of material particles would appear to make a rigorous solution of the problem difficult. However, an approximate solution was obtained by Hertz when he assumed that the stresses and strains near the contact region may be computed as though the contact was static [1]. The solution is considered valid for moderate impact velocities.

In an earlier work [2], the fractures produced in glass blocks by the impact of steel balls were studied by observing the fracture stress waves and varying the impact velocity. At highest velocities of impact, the recorded stress waves showed that fractures occurred only a few microseconds after the glass blocks were first compressed. At the instant of fracture, the rate of increase in dynamic loading and the contact area was large, phenomena which raise questions about the validity of the Hertz impact theory for determining stresses at that state of loading.

Tsai [3] recently studied the contact stress distribution in an elastic plate of finite thickness subjected to the indentations of spherical indenters on the upper and lower surfaces of the plate. The ratio of the maximum tensile stress in the plate to the corresponding half-space value was shown to approach unity for thick plates, but to increase with decreasing plate thickness. This magnification of the maximum tensile stress in thin plates was demonstrated experimentally [4]. In considering the associated dynamic problems, questions again arise about the conditions under which the results obtained by Tsai can be extended to the dynamic case as Hertz did in his impact theory.

In the work described here, the dynamic contact stresses between an axisymmetric projectile and an elastic half-space are studied by solving the three-dimensional equations

of motion. These stresses are written as the sum of the Hertz contact stresses and the effect of stress waves. To study the validity of the conventional impact theory, the stresses determined here are compared with those predicted by the Hertz theory in terms of contact time and contact radius.

2. DYNAMIC CONTACT STRESS

Consider an elastic half-space subjected to the impact of a rigid, axisymmetric projectile. Assume that during impact the axis of symmetry of the projectile is perpendicular to the free surface. The problem is now axisymmetric, and the response of a half-space to dynamic surface loadings can be studied by Hankel transforms [2, 5, 6]. For the problem considered here, it is assumed that the shear stress vanishes on the free surface and that during impact the normal contact stress between the projectile and the half-space, $p(r, t)$, is a function of radial distance r and time t. In fact, $p(r, t)$ can be determined as the solution to an integral equation. During impact, the contact area between the projectile and the half-space $a(t)$ generally varies with time. Thus the problem has moving boundary conditions with a finite loading area. To solve the problem, Hankel transforms are first applied over r, and Laplace transforms are operated over t. From the results obtained by Tsai [5], it can be induced that on the free surface, $z = 0$, the Laplace transform of the vertical displacement is

$$U_z^*(r, p) = -\frac{1}{\mu}\int_0^\infty k_2 \bar{p}^*(s, p) F^*(s, p) J_0(sr)\, ds, \tag{1}$$

where

$$\bar{p}(s, t) = \int_0^{a(t)} p(r, t) J_0(rs) r\, dr, \quad \bar{p}^* = \int_0^\infty e^{-pt}\bar{p}(s, t)\, dt \tag{2}$$

$$F^*(s, p) = \frac{s k_2 (s^2 + k_1^2)^{\frac{1}{2}}}{(2s^2 + k_2^2)^2 - 4s^2(s^2 + k_1^2)^{\frac{1}{2}}(s^2 + k_2^2)^{\frac{1}{2}}} \tag{3}$$

$$k_1 = \frac{p}{c_1}, \qquad k_2 = \frac{p}{c_2}, \qquad c_1^2 = \frac{(\lambda + 2\mu)}{\rho}, \qquad c_2^2 = \frac{\mu}{\rho} \tag{4}$$

The Laplace inversion of (1) can be obtained by considering $F^*(s, p)$ as the transform of $f(s, t)$. To obtain the inversion of (3), let $p = sc_2\zeta$ and cut the complex ζ-plane as shown in Fig. 1. The inversion of (3) is

$$\begin{aligned} f(s, t) &= \frac{1}{2\pi i}\int_{\delta - i\infty}^{\delta + i\infty} F^*(s, p)\, e^{pt}\, dp \\ &= \frac{c_2}{2\pi i}\int_{\delta - i\infty}^{\delta + i\infty} \frac{\zeta(1 + \zeta^2/k^2)^{\frac{1}{2}}\, e^{c_2 s\zeta t}}{g(\zeta)}\, d\zeta, \end{aligned} \tag{5}$$

where

$$k^2 = \frac{k_2^2}{k_1^2} = \frac{2(1 - \nu)}{1 - 2\nu} \tag{6}$$

$$g(\zeta) = (2 + \zeta^2)^2 - 4\left[\left(1 + \frac{\zeta^2}{k^2}\right)(1 + \zeta^2)\right]^{\frac{1}{2}}. \tag{7}$$

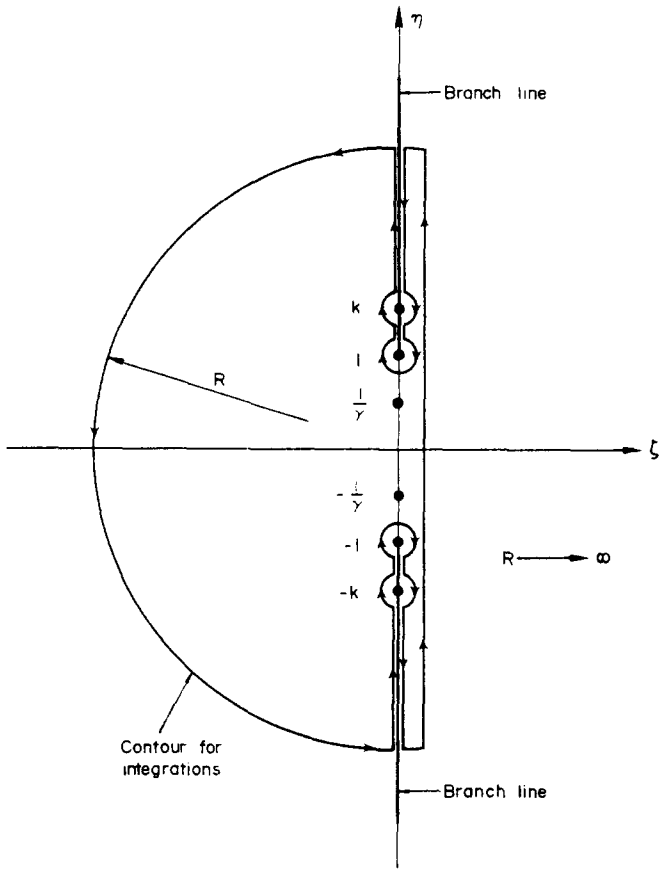

FIG. 1. Contour for integrations.

Around the origin $\zeta = 0$, (7) has the expansion

$$g(\zeta) = \frac{1}{1-v}\zeta^2 + 0(\zeta^3). \tag{8}$$

Therefore, the integrand of (5) has a simple pole at $\zeta = 0$. In addition $g(\zeta)$ has poles at $\zeta = \pm i(1/\gamma)$ which give the Rayleigh wave speed. The value of γ depends on Poisson's ratio v. Integration of (5) along the contour in Fig. 1 gives

$$f(s, t) = c_2[(1-v)H(t) + L\cos(c_2\eta st)], \tag{9}$$

where $H(t)$ is the Heaveside function, and the operator is

$$\begin{aligned} L\cos(c_2\eta st) = {} & \frac{2(1-1/\gamma^2k^2)^{\frac{1}{2}}}{\gamma g'(\gamma)}\cos\left\{\frac{c_2 st}{\gamma}\right\} \\ & -\frac{8}{\pi}\int_1^k \frac{(1-\eta^2/k^2)(\eta^2-1)^{\frac{1}{2}}\eta\cos(c_2 s\eta t)}{(2-\eta^2)^4 + 16(1-\eta^2/k_2)(\eta^2-1)}\,d\eta \\ & -\frac{2}{\pi}\int_k^\infty \frac{[(\eta^2/k^2)-1]^{\frac{1}{2}}\eta\cos(c_2 s\eta t)}{(2-\eta^2)^2 + 4\{[(\eta^2/k^2)-1](\eta^2-1)\}^{\frac{1}{2}}}\,d\eta \end{aligned} \tag{10}$$

and

$$g'(\gamma) = -i\frac{\partial g}{\partial \zeta} \text{ at } \zeta = i\frac{1}{\gamma}. \tag{11}$$

The first term in (9) is the contribution of the pole at $\zeta = 0$. In (10) the first term is the contribution of the poles at $\zeta = \pm i(1/\gamma)$; the other terms result from the branch cuts. The expression and intervals of integration in (10) are similar to those obtained in Refs. [5, 7, 8] for vertical displacements. If equation (1) is divided by k_2, the inversion of that gives

$$\int_0^t u_z(r, \tau)\,\mathrm{d}\tau = -\frac{1-\nu}{\mu}\int_0^\infty J_0(sr)\int_0^t \bar{p}(s, \tau)\,\mathrm{d}\tau\,\mathrm{d}s$$

$$-\frac{1}{\mu}L\int_0^\infty J_0(sr)\int_0^t \cos[c_2\eta s(t-\tau)]\bar{p}(s, \tau)\,\mathrm{d}\tau\,\mathrm{d}s. \tag{12}$$

Equation (12) is now suitable for determining the dynamic contact stress $p(r, t)$. To find $p(r, t)$, assume the vertical displacement produced by the projectile inside the contact area can be described by $g(r, t)$, i.e. $u_z(r, t) = g(r, t)$ for $r \le a(t)$ at $z = 0$. For projectiles of simple geometry, $g(r, t)$ can generally be determined. Equation (12) now becomes an integral equation with the unknown $p(r, t)$. When inverting (12), the orders of integration or differentiation are important in order to avoid unmanageable singularities. Applying some integral identities [3, 9, 10] to (12) gives

$$\frac{\partial}{\partial r}\int_0^r \frac{m\,\mathrm{d}m}{(r^2-m^2)^{\frac{1}{2}}}\int_0^t g(m, \tau)\,\mathrm{d}\tau$$

$$= -\frac{1-\nu}{\mu}\int_0^t\int_0^{a(\tau)} p(\lambda, \tau)\lambda\frac{H(\lambda-r)}{(\lambda^2-r^2)^{\frac{1}{2}}}\,\mathrm{d}\lambda\,\mathrm{d}\tau - \frac{1}{2\mu}W(r, t), \tag{13}$$

where

$$W(r, t) = L\int_0^t\int_0^{a(\tau)} p(\lambda, \tau)\lambda\left\{\frac{H[\lambda-|r-b(t-\tau)|]}{[\lambda^2-[r-b(t-\tau)]^2]^{\frac{1}{2}}}\right.$$

$$\left.+\frac{H[\lambda-|r+b(t-\tau)|]}{[\lambda^2-[r+b(t-\tau)]^2]^{\frac{1}{2}}}\right\}\mathrm{d}\lambda\,\mathrm{d}\tau \tag{14}$$

and

$$b = c_2\eta.$$

On the right side of (13), the first integral is similar to the corresponding term obtained in the static case while the second integral, i.e. (14), is due to wave effects which obviously do not occur in static problems. The domain of influence of stress waves which is the integration region of (14) is shown by the hatched portion in Fig. 2. The hatched area applies to the first term in (14) while the second term is integrated only over the cross-hatched region. For future convenience, the dot and prime will indicate differentiations with respect to

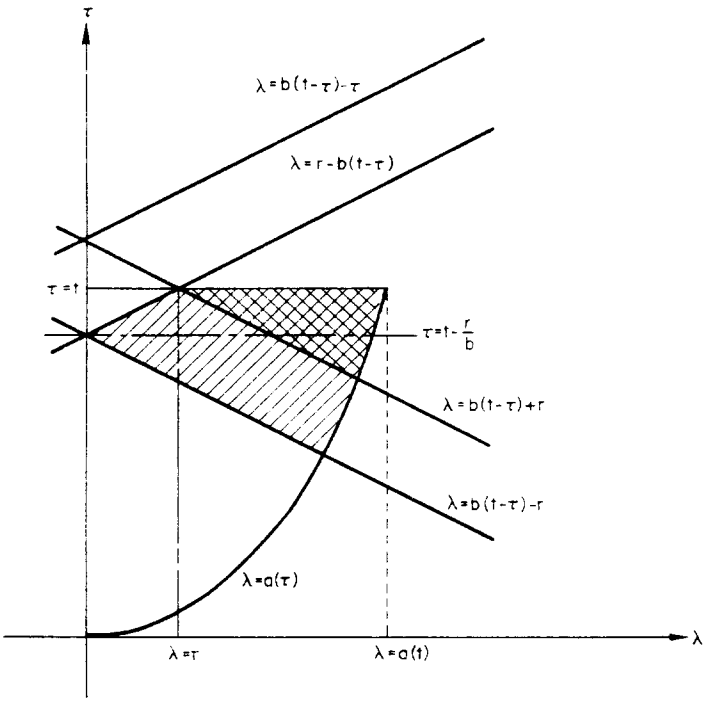

FIG. 2. Regions of integrations.

time and space respectively. The following wave functions are defined:

$$G_1 = \frac{1}{\{\lambda^2-[r-b(t-\tau)]^2\}^{\frac{1}{2}}},$$

$$G_2 = \frac{1}{\{\lambda^2-[b(t-\tau)-r]^2\}^{\frac{1}{2}}},$$

$$G_3 = \frac{1}{\{\lambda^2-[b(t-\tau)+r]^2\}^{\frac{1}{2}}}, \tag{15}$$

Integrating over the hatched region in Fig. 2 and assuming the normal stress vanishes on the boundary of the contact area, i.e. $p[a(t), t] = 0$, (14) gives

$$\frac{\partial W(r,t)}{\partial t} = L\left\{\int_r^{a(t)} \frac{\partial}{\partial t}\left[\int_{t-r/b}^{t} G_1 p(\lambda,\tau)\,d\tau + \int_{t-[(\lambda+r)/b]}^{t-r/b} G_2 p(\lambda,\tau)\,d\tau + \int_{t-[(\lambda-r)/b]}^{t} G_3 p(\lambda,\tau)\,d\tau\right]\lambda\,d\lambda + \int_0^r \frac{\partial}{\partial t}\left[\int_{t-r/b}^{t-[(r-\lambda)/b]} G_1 p(\lambda,\tau)\,d\tau + \int_{t-[(\lambda+r)/b]}^{t-r/b} G_2 p(\lambda,\tau)\,d\tau\right]\lambda\,d\lambda\right\}. \tag{16}$$

To invert (13), the following integration by parts on (16) is required:

$$\int_r^{a(t)} \frac{\xi W(\xi, t)/\partial t}{(\xi^2 - r^2)^{\frac{1}{2}}}\,d\xi = (a^2 - r^2)^{\frac{1}{2}} \frac{\partial W[a(t), t]}{\partial t} - \int_r^{a(t)} (\xi^2 - r^2)^{\frac{1}{2}} \frac{\partial^2 W(\xi, t)}{d\xi \partial t}\,d\xi \tag{17}$$

where

$$\begin{aligned}\frac{\partial W[a(t), t]}{\partial t} &= L \int_0^{a(t)} \frac{\partial}{\partial t} \int_{t-[a(t)/b]}^{t-|[a(t)-\lambda]/b|} \frac{p(\lambda, \tau)\lambda\,d\lambda\,d\tau}{\{\lambda^2 - [a(t) - b(t-\tau)]^2\}^{\frac{1}{2}}} \\ &\quad + L \int_0^{a(t)} \frac{\partial}{\partial t} \int_{t-|[a(t)+\lambda]/b|}^{t-[a(t)/b]} \frac{p(\lambda, \tau)\lambda\,d\lambda\,d\tau}{\{\lambda^2 - [b(t-\tau) - a(t)]^2\}^{\frac{1}{2}}} \\ &= -L\left\{\int_{t-[a(t)/b]}^{t} \int_{a(t)-b(t-\tau)}^{a(\tau)} \frac{[\partial p(\lambda, \tau)/\partial\tau]\lambda\,d\lambda}{\{\lambda^2 - [a(t) - b(t-\tau)]^2\}^{\frac{1}{2}}}\,d\tau,\right. \\ &\quad \left. + \int_{t^*}^{t-[a(t)/b]} \int_{b(t-\tau)-a(t)}^{a(\tau)} \frac{[\partial p(\lambda, \tau)/\partial\tau]\lambda\,d\lambda}{\{\lambda^2 - [b(t-\tau) - a(t)]^2\}^{\frac{1}{2}}}\,d\tau\right\},\end{aligned}$$

$$t^* = t - \frac{a(t) + a(t^*)}{b}. \tag{18}$$

Now (13) gives

$$\begin{aligned}&\frac{\partial}{\partial r} \int_r^{a(t)} \frac{\xi\,d\xi}{(\xi^2 - r^2)^{\frac{1}{2}}} \frac{\partial}{\partial \xi} \int_0^{\xi} \frac{m[g(m, t)]\,dm}{(\xi^2 - m^2)^{\frac{1}{2}}} \\ &\quad = \frac{1 - \nu}{\mu} r[p(r, t)] \frac{\pi}{2} + \frac{r}{(a^2 - r^2)^{\frac{1}{2}}} \frac{\partial W[a(t), t]}{2\mu \partial t} - \frac{1}{2\mu} \int_r^{a(t)} \frac{r}{(\xi^2 - r^2)^{\frac{1}{2}}} \frac{\partial^2 W(\xi, t)}{\partial \xi \partial t}\,d\xi.\end{aligned} \tag{19}$$

Equation (19) results in the following two equations:

$$\begin{aligned}p(r, t) &= \frac{2\mu}{(1 - \nu)\pi} \int_r^{a(t)} \frac{d\xi}{(\xi^2 - r^2)^{\frac{1}{2}}} \frac{\partial}{\partial \xi} \int_0^{\xi} \frac{\xi[g'(m, t)]\,dm}{(\xi^2 - m^2)^{\frac{1}{2}}} \\ &\quad + \frac{1}{(1 - \nu)\pi} \int_r^{a(t)} \frac{1}{(\xi^2 - r^2)^{\frac{1}{2}}} \frac{\partial^2 W(\xi, t)}{\partial \xi \partial t}\,d\xi\end{aligned} \tag{20}$$

and

$$g(0, t) + a(t) \int_0^{a(t)} \frac{g'(m, t)\,dm}{(a^2 - m^2)^{\frac{1}{2}}} + \frac{\partial W[a(t), t]}{2\mu \partial t} = 0. \tag{21}$$

Equation (20) can be used to determine the normal contact stress $p(r, t)$ while (21) relates the distance of approach $g(0, t)$ to the radius of the contact region $a(t)$. The terms involving $W(\xi, t)$ in (20) and (21) represent stress wave effects. If these terms are dropped, (20) and (21) reduce to the corresponding static equations. By integration by parts over z, differentiation with respect to t and finally changing the orders of integration, (16) can be simplified as

$$\begin{aligned}\frac{\partial W(r, t)}{\partial t} &= -L\left\{\int_{t-r/b}^{t} \int_{r-b(t-\tau)}^{a(\tau)} G_1 \dot{p}(\lambda, \tau)\lambda\,d\lambda\,d\tau\right. \\ &\quad + \int_{t_1}^{t-r/b} \int_{b(t-\tau)-r}^{a(\tau)} G_2 \dot{p}(\lambda, \tau)\lambda\,d\lambda\,d\tau \\ &\quad \left. + \int_{t_2}^{t} \int_{b(t-\tau)+r}^{a(\tau)} G_3 \dot{p}(\lambda, \tau)\lambda\,d\lambda\,d\tau\right\}.\end{aligned} \tag{22}$$

where

$$t_1 = t - \frac{a(t_1) + r}{b}. \tag{23}$$

$$t_2 = t - \frac{a(t_2) - r}{b}. \tag{24}$$

Equations (20) and (21) are sufficient to solve the static contact problem [3, 9]. However, for the dynamic problem considered here, an additional equation relating projectile mass to reaction of the half-space is required. Thus from Newton's law

$$m\ddot{g}(0, t) = -P(t) = -2\pi \int_0^{a(t)} p(r, t) r \, dr. \tag{25}$$

The system of the three integral–differential equations (20), (21) and (25) is now sufficient to determine the dynamic unknowns $p(r, t)$, $a(t)$ and $g(0, t)$. The problem is well defined. However, the solution for a particular problem depends on the function $g(r, t)$, which is associated with the shape of a projectile.

The solution for the impact of a spherical body with radius R or a projectile with round end of radius R will now be discussed in detail. For these projectiles, the shape of penetration can be written as [3, 9]

$$g(r, t) = \alpha(t) - \frac{r^2}{2R} H(t), \tag{26}$$

where $g(0, t) = \alpha(t)$ is the distance of approach occurring at the center of the contact region. The three coupled equations (20), (21) and (25) will now be studied by successive approximations. Substituting (26) into (20) and (21) and dropping the wave-effect functions, the first approximation solutions are

$$p(r, t) = -\frac{4\mu}{(1-\nu)\pi R} [a(t)^2 - r^2]^{\frac{1}{2}} \tag{27}$$

and

$$\alpha(t) = \frac{a(t)^2}{R}. \tag{28}$$

Although a and α are functions of time, (27) and (28) are precisely the results obtained in static half-space contact problems [3, 9]. Integrating (27) over r gives the total force

$$P(t) = -\frac{8\mu}{3R(1-\nu)} a(t)^3. \tag{29}$$

In terms of (26) and (29), equation (25) can be integrated to obtain the relationship between α and t. It was shown [11, 12] that $\alpha(t)$ can be approximated by $\alpha(t) = 0{\cdot}995\alpha_1 \sin(\pi t/T)$, where α_1 is the maximum distance of approach and T is the duration of contact. In terms of $\alpha(t)$ and (28), the radius of contact is

$$a(t) = (0{\cdot}995)^{\frac{1}{2}} a_1 \sin^{\frac{1}{2}}\left(\frac{\pi t}{T}\right), \tag{30}$$

where the maximum radius of contact in terms of the impact velocity V is

$$a_1^5 = \alpha_1^{5/2} R^{5/2} = \frac{15(1-\nu)m}{32\mu} R^2 V^2. \tag{31}$$

Equations (27)–(31) are predicted in the Hertz theory [1].

To find the second approximation for $p(r, t)$, (27) is substituted into (20) and (22). All the integrations over λ in (22) result in $\pi/2$. Therefore, (20) and (22) give

$$p(r,t) = -\frac{4\mu}{(1-\nu)\pi R}\left\{[a^2(t)-r^2]^{\frac{1}{2}} - \frac{1}{2(1-\nu)} L \int_r^{a(t)} \frac{1}{(\xi^2-r^2)^{\frac{1}{2}}}\left[\frac{a(t_1)\dot{a}(t_1)}{b+\dot{a}(t_1)} - \frac{a(t_2)\dot{a}(t_2)}{b+\dot{a}(t_2)}\right] d\xi\right\}. \tag{32}$$

Without solving (32) explicitly, some general results can be obtained. The quantities in the second bracket of (32) which are defined in (23) and (24) depend on wave speeds and the value and rate of increase of the contact area. The values of $a(t)$ and $\dot{a}(t)$ are functions of R and T which in turn depend on V. The larger the impact velocity V, the shorter the contact time T. For moderate impact velocity, T is large and the time needed for waves to traverse the contact area is very short compared to T. For this case, it can be seen from Fig. 2 that the values for t, t_1 and t_2 are very near each other. Therefore, the value inside the second bracket of (32) must be quite small. Hence, the dynamic contact stress $p(r, t)$ in (32) can be approximated by the first term which is precisely the value used in the Hertz theory of impact [1].

The total impact force can be determined by integrating (32) over r. Thus,

$$P(t) = 2\pi \int_0^{a(t)} p(r,t) r \, dr = -\frac{8\mu}{(1-\nu)R}\left\{\frac{a^3}{3} - \frac{L}{2(1-\nu)} \int_0^{a(t)} \left[\frac{a(t_1)\dot{a}(t_1)}{b+\dot{a}(t_1)} - \frac{a(t_2)\dot{a}(t_2)}{b+\dot{a}(t_2)}\right] \xi \, d\xi\right\}. \tag{33}$$

Equations (32) and (33) require the determinations of $a(t_1)$ and $a(t_2)$. These values are determined if the Rayleigh wave front exceeds the contact circle. For extremely small t, the normal stress and total force can be obtained from (1) for large values of p. Indeed, (1) can be written for large p as

$$U_z^*(r,p) = -\frac{1}{\rho c_1 p} \int_0^r s\bar{p}^* J_0(sr) \, ds.$$

The inversion is

$$\alpha(t) - \frac{r^2}{2R} H(t) = -\frac{1}{\rho c_1} \int_0^r s \int_0^t \bar{p}(s,\tau) \, d\tau J_0(sr) \, ds$$

For small t, $\alpha(t)$ is equal to Vt. Differentiating the above equation with respect to t gives

$$p(r,t) = -\rho c_1 V \text{ for } r \le a(t) \text{ and } t > 0.$$

Integrating over the area of contact gives

$$P(t) = -\rho c_1 V A(t)$$

where the contact area $A = \pi a^2$. The above simple expression is the same as that obtained by Thompson and Robinson [16].

3. RADIAL SURFACE STRESS

The tensile radial surface stress, which is the critical stress in the study of fractures in Ref. [2], can also be calculated from the solutions for three-dimensional equations of motion. From the results obtained by Tsai [5], the Laplace transform of the vertical and radial displacements can be written as

$$U_z^* = -\frac{1}{\mu}\int_0^\infty \frac{\bar{p}^* s\alpha[(k_2^2+2s^2)\,e^{-\alpha z} - 2s^2\,e^{-\beta z}]J_0(sr)\,ds}{(k_2^2+2s^2)^2 - 4s^2\alpha\beta} \tag{34}$$

and

$$U_r^* = -\frac{1}{\mu}\int_0^\infty \frac{\bar{p}^* s^2[(k_2^2+2s^2)\,e^{-\alpha z} - 2\alpha\beta\,e^{-\beta z}]J_1(sr)\,ds}{(k_2^2+2s^2)^2 - 4s^2\alpha\beta}. \tag{35}$$

where $\alpha = (s^2+k_1^2)^{\frac{1}{2}}$ and $\beta = (s^2+k_2^2)^{\frac{1}{2}}$.

In terms of the above displacements, the transform of the radial stress on the free surface can be written as

$$\begin{aligned}\sigma_{rr}^* &= 2\int_0^\infty \frac{\bar{p}^* s^2[(k_2^2+2s^2)-2\alpha\beta]}{(k_2^2+2s^2)^2-4s^2\alpha\beta}\left[\frac{J_1(sr)}{r} - sJ_0(sr)\right]ds \\ &\quad + \frac{\nu}{1-\nu}\int_0^\infty \frac{\bar{p}^* s k_2^2(k_2^2+2s^2)J_0(sr)\,ds}{(k_2^2+2s^2)^2-4s^2\alpha\beta} \\ &= \int_0^\infty \bar{p}^*\left[\frac{J_1(sr)}{r} - sJ_0(sr)\right]ds \\ &\quad - k_2\int_0^\infty \bar{p}^*\bar{F}(s,p)\left[\frac{J_1(sr)}{r} - \frac{1}{1-\nu}sJ_0(sr)\right]ds,\end{aligned} \tag{36}$$

where

$$\bar{F} = \frac{k_2(2s^2+k_2^2)}{(2s^2+k_2^2)^2 - 4s^2\alpha\beta}. \tag{37}$$

The above $\bar{F}$ can be considered as a transform function, and its inversion can be obtained by integrating along the contour shown in Fig. 1. Similar to (9), the result is

$$f(s,t) = \frac{1}{2\pi i}\int_{\delta-i\infty}^{\delta+i\infty} \bar{F}(s,p)\,e^{pt}\,dp = c_2[2(1-\nu)H(t) + \bar{L}\cos(sbt)], \tag{38}$$

where the operator is

$$\begin{aligned}\bar{L}\cos(sbt) &= \frac{2(2-1/\gamma^2)}{g(\gamma)}\cos\left(\frac{sc_2 t}{\gamma}\right) \\ &\quad - \frac{8}{\pi}\int_1^k \frac{(\eta^2-1)^{\frac{1}{2}}(1-\eta^2/k^2)^{\frac{1}{2}}\eta(2-\eta^2)\cos(sc_2\eta t)}{(2-\eta^2)^4 + 16(\eta^2-1)(1-\eta^2/k^2)}\,d\eta.\end{aligned} \tag{39}$$

Dividing equation (36) by k_2 and using (38), the inversion of (36) is

$$\int_0^t \sigma_{rr}(r,\tau)\,d\tau = \int_0^t\int_0^\infty \bar{p}(s,\tau)sJ_0(sr)\,ds$$
$$-(1-2\nu)\int_0^t\int_0^\infty \bar{p}(s,\tau)\frac{J_1(sr)}{r}\,ds - Q_1(t,r)+Q_2(t,r)$$
$$= \int_0^t p(r,\tau)\,d\tau-(1-2\nu)\frac{1}{r^2}\int_0^t\int_0^r p(\lambda,\tau)\lambda\,d\lambda\,d\tau$$
$$-Q_1(t,r)+Q_2(t,r), \tag{40}$$

where

$$Q_1(t,r) = \bar{L}\int_0^t\int_0^\infty \cos[sb(t-\tau)]\bar{p}(s,\tau)\frac{J_1(sr)}{r}\,ds\,d\tau \tag{41}$$

and

$$Q_2(t,r) = \frac{1}{1-\nu}\bar{L}\int_0^t\int_0^\infty \cos[sb(t-\tau)]\bar{p}(s,\tau)sJ_0(sr)\,ds\,d\tau. \tag{42}$$

Applying Abel's transform to (42) gives

$$\bar{Q}_2(t,x) = \int_0^x \frac{\xi Q_2(t,\xi)\,d\xi}{(x^2-\xi^2)^{\frac{1}{2}}} = \frac{1}{1-\nu}\bar{L}\int_0^t\int_0^\infty \bar{p}(s,\tau)\tfrac{1}{2}\{\sin s[x+b(t-\tau)]$$
$$+\sin s[x-b(t-\tau)]\}\,ds = \frac{1}{2(1-\nu)}I(t,x), \tag{43}$$

where

$$I(t,r) = \bar{L}\int_0^t\int_0^{a(\tau)} p(\lambda,\tau)\lambda\,d\lambda\left\{\frac{H[|r+b(t-\tau)|-\lambda]}{\{[r+b(t-\tau)]^2-\lambda^2\}^{\frac{1}{2}}}+\frac{H[|r-b(t-\tau)|-\lambda]}{\{[r-b(t-\tau)]^2-\lambda^2\}^{\frac{1}{2}}}\right\}d\tau. \tag{44}$$

If Abel's transform and its inversion are successively carried out over (40), it becomes

$$\int_0^t \sigma_{rr}(r,\tau)\,d\tau = \int_0^t p(r,\tau)\,d\tau-(1-2\nu)\frac{1}{r^2}\int_0^t\int_0^r p(\lambda,\tau)\lambda\,d\lambda\,d\tau$$
$$-Q_1(t,r)+\frac{1}{1-\nu}\frac{1}{\pi r}\frac{\partial}{\partial r}\int_0^r \frac{xI(t,x)\,dx}{(r^2-x^2)^{\frac{1}{2}}}. \tag{45}$$

If the identity

$$\frac{\partial}{\partial r}\int_0^r \frac{J_1(sm)}{m}\frac{m^3\,dm}{(r^2-m^2)^{\frac{1}{2}}} = r\sin(sr)$$

is used, (41) gives

$$\frac{\partial}{\partial r}\int_0^r \frac{m^3Q_1(t,m)\,dm}{(r^2-m^2)^{\frac{1}{2}}} = \frac{r}{2}I(t,r). \tag{46}$$

Then

$$\int_0^r \frac{\mathrm{d}\xi}{(r^2-\xi^2)^{\frac{1}{2}}} \frac{\partial}{\partial \xi} \int_0^{\xi} \frac{m^3 f(t, m)\,\mathrm{d}m}{(r^2-m^2)^{\frac{1}{2}}} = \frac{\pi}{2} r^2 f(t, r). \tag{47}$$

If the operations on the left side of (47) are applied to (45) which is then differentiated with respect to time. the result is

$$\sigma_{rr}(r, t) = p(r, t) - (1-2\nu)\frac{1}{r^2}\int_0^r p(\lambda, t)\lambda\,\mathrm{d}\lambda - \frac{\partial \overline{W}}{\partial t}, \tag{48}$$

where

$$\overline{W} = \frac{1}{\pi r^2}\int_0^r \frac{xI(t, x)\,\mathrm{d}x}{(r^2-x^2)^{\frac{1}{2}}} - \frac{1}{1-\nu}\frac{1}{\pi r}\frac{\partial}{\partial r}\int_0^r \frac{xI(t, x)\,\mathrm{d}x}{(r^2-x^2)^{\frac{1}{2}}}. \tag{49}$$

The first two terms on the right side of (48) are predicted in the Hertz impact theory. The third term, which is new here, is due to wave effects.

The region of integration for the first term of (44) is outside the hatched area in Fig. 2; that for the second term of (44) is outside the cross-hatched area. If the following wave functions are introduced

$$\begin{aligned} \bar{G}_1 &= \frac{1}{\{[x-b(t-\tau)]^2-\lambda^2\}^{\frac{1}{2}}}, \\ \bar{G}_2 &= \frac{1}{\{[b(t-\tau)-x]^2-\lambda^2\}^{\frac{1}{2}}}, \\ \bar{G}_3 &= \frac{1}{\{[b(t-\tau)+x]^2-\lambda^2\}^{\frac{1}{2}}}, \end{aligned} \tag{50}$$

(44) can be written

$$\begin{aligned} I(t, r) = \bar{L}\Bigg\{ &\int_{t-x/b}^{t}\int_0^{x-b(t-\tau)} \bar{G}_1 p(\lambda, \tau)\lambda\,\mathrm{d}\lambda\,\mathrm{d}\tau \\ &- \int_{t_1}^{t-x/b}\int_0^{b(t-\tau)-x} \bar{G}_2 p(\lambda, \tau)\lambda\,\mathrm{d}\lambda\,\mathrm{d}\tau - \int_0^{t_1}\int_0^{a(\tau)} \bar{G}_2 p(\lambda, \tau)\lambda\,\mathrm{d}\lambda\,\mathrm{d}\tau \\ &+ \int_{t_2}^{t}\int_0^{b(t-\tau)+x} \bar{G}_3 p(\lambda, \tau)\lambda\,\mathrm{d}\lambda\,\mathrm{d}\tau + \int_0^{t_2}\int_0^{a(\tau)} \bar{G}_3 p(\lambda, \tau)\lambda\,\mathrm{d}\lambda\,\mathrm{d}\tau\Bigg\}. \end{aligned} \tag{51}$$

This equation is suitable for numerical integration; integration of (48) will be discussed in the next section.

4. NUMERICAL INTEGRATIONS AND RESULTS

Both the normal contact stress $p(r, t)$ and the surface radial stress $\sigma_{rr}(r, t)$ are written in (32) and (48) respectively as the sums of the corresponding quantities predicted by the Hertz theory and wave-effect integrals. The integrands of these integrals involve singularities in either the upper or lower limits of integration. The difficulties of dealing with singular integrands can be overcome by using the methods of product-integration [13, 14]. Using

this technique, two four-point integration formulae needed in equations (50) and (51) are developed in Appendix A. Formula I is used in (32) while Formula II is used in (48). For integrations not involving singularities, common three-point or four-point methods are used. The differentiations in (48) and (49) are performed by the Lagrange method [15]. Five points are calculated for each differentiation, and the point of differentiation needed is an interior point of the interval over which the results are smooth.

The value of the surface radial stress $\sigma_{rr}[a(t), t]$ along the circle of contact is calculated for various values of maximum contact radius a and contact time T, as shown in Figs. 3 (a and b). The curves show the ratio between the radial stress $\sigma_{rr}[a(t), t]$ obtained here by considering the wave effect and the corresponding value predicted by the Hertz theory, which is the sum of the first two terms in (48). Figure 3(a) shows the ratio at 1 μsec after projectiles first press the material; Fig. 3(b) shows the ratio during the middle of the impact, $t = T/2$. At $t = 1$ μsec the ratio increases rapidly with increasing a_1 and decreasing T, as shown in Fig. 3(a). At $t = T/2$, however, the curves in Fig. 3(b) show that the ratio decreases if a_1 increases and T decreases. For relatively small a_1 and large T, both curves approach unity where the Hertz theory applies.

The value of the dynamic normal contact stress $p(r, t)$ can be calculated from (32) for all values of r inside the contact circle except for the point $r = 0$. By choosing a value of r sufficiently close to zero and other values of r less than $a(t)$, the shape of $p(r, t)$ is determined by a computer. The integration of $p(r, t)$ in (33) gives the value of the total dynamic force $P(t)$. The values of the ratio between $P(t)$ predicted here and the corresponding value obtained in the Hertz theory are calculated for various values of a_1 and T. The results tabulated in Appendix B show there is only a very small difference between the present theory and

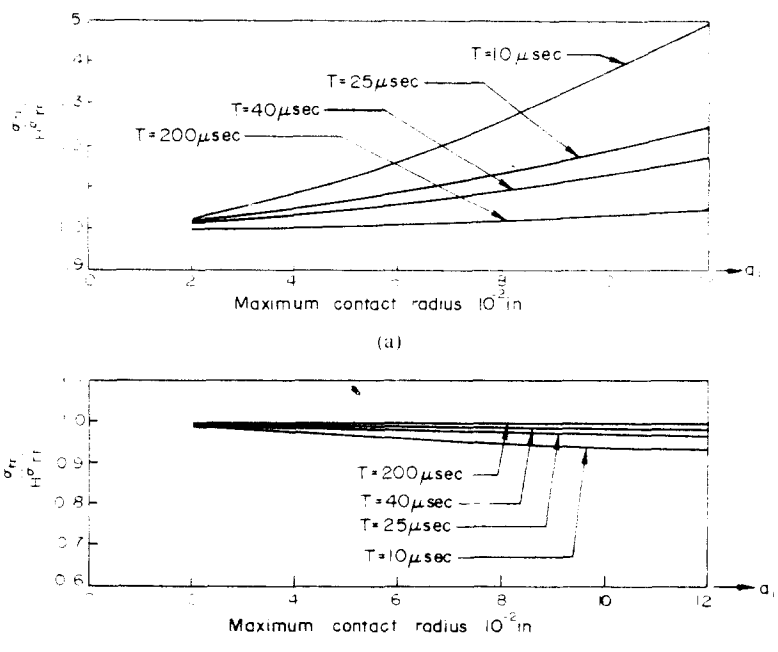

FIG. 3. Radial contact stresses $\sigma_{rr}[a(t), t]$ normalized by the corresponding Hertz stresses $\mu\sigma_{rr}[a(t), t]$ (a) $t = 1$ μsec; (b) $t = T/2$.

that of Hertz. A similar situation for $p(r, t)$ is also indicated in the results obtained from computations.

5. CONCLUSION

By using integral transforms to solve three-dimensional equations of motion and the techniques used by Young and Linz [13, 14], the normal contact stress and radial surface stress caused by impact of an axisymmetric projectile on an elastic half-space can be written as the sums of the corresponding Hertz contact stresses and wave-effect integrals. The singular integrands can be numerically integrated using the product-integration technique. The contact stresses are calculated for various values of the contact time T and the maximum contact radius a_1. The Hertz theory is a good approximation for determining the total force produced by the projectile. However, in calculating the maximum radial surface stress when the contact radius is maximum, the Hertz theory applies only for moderate impact velocities where the contact time is more than approximately 40 μsec.

The discrepancy between the Hertz radial stress and the corresponding value obtained here increases with decreasing contact time and increasing contact radius. The discrepancy is larger at 1 μsec after the projectile first presses the material than at the middle of the contact time.

Acknowledgements—The author wishes to express his appreciation for the financial support of the National Science Foundation through Research Initiation Grant (GK-4671) and the Engineering Research Institute, Iowa State University, Ames, Iowa.

REFERENCES

[1] A. E. H. LOVE, *A Treatise of Mathematical Theory of Elasticity*, p. 198. Dover (1944).
[2] Y. M. TSAI and H. KOLSKY, A study of the fractures produced in glass blocks by impact. *J. Mech. Phys. Solids* **15**, 263–278 (1967).
[3] Y. M. TSAI, Stress distribution in elastic and viscoelastic plates subjected to symmetrical rigid indentations. *Q. appl. Math.* **27**, 371–380 (1969).
[4] Y. M. TSAI, Thickness dependence of the indentation hardness of glass plates. *Int. J. Fracture Mech.* **5**, 157–165 (1969).
[5] Y. M. TSAI, Stress waves produced by impact on the surface of a plastic medium. *J. Franklin Inst.* **285**, 204–221 (1968).
[6] Y. M. TSAI and H. KOLSKY, Surface wave propagation for linear viscoelastic solids. *J. Mech. Phys. Solids* **16**, 99–109 (1968).
[7] C. L. PEKERIS, The seismic surface pulse. *Proc. natn. Acad. Sci. U.S.A.* **41**, 469–480 (1955).
[8] H. LAMB, On the propagation of tremors over the surface of an elastic solid. *Phil. Trans. R. Soc.* **A203**, 1–42 (1904).
[9] T. C. T. TING, The contact stresses between a rigid indenter and a viscoelastic half-space. *J. appl. Mech.* **4**, 845–854 (1966).
[10] G. N. WATSON, *A Treatise on the Theory of Bessel Functions*, 2nd edition, p. 405. Cambridge University Press (1944).
[11] S. C. HUNTER, Energy absorbed by elastic waves during impact. *J. Mech. Phys. Solids* **5**, 162–171 (1957).
[12] Y. M. TSAI, A note on the surface waves produced by Hertzian impact. *J. Mech. Phys. Solids* **16**, 133–136 (1968).
[13] A. YOUNG, Approximate product-integration. *Proc. R. Soc.* **A224**, 552–573 (1954).
[14] P. LINZ, Applications of Abel Transforms to the Numerical Solution of Problems in Electrostatics and Elasticity. Mathematics Research Center Report, University of Wisconsin (1967).
[15] K. S. KUNZ, *Numerical Analysis*, p. 86. McGraw-Hill (1957).
[16] J. C. THOMPSON and A. R. ROBINSON, Exact Solutions of Some Dynamic Problems of Indentation and Transient Loadings of an Elastic Half Space. Structural Research Series No. 350, Civil Engineering Studies, University of Illinois, Urbana (1969).

APPENDIX A

Product-integration formulae

Formula I.

$$\int_{r_1}^{r_4} f(\xi)\phi(\xi, r)\,d\xi = \alpha_1 f(r_1)+\alpha_2 f(r_1+\Delta r)+\alpha_3 f(r_1+2\Delta r)$$

$$+\alpha_4 f(r_1+3\Delta r),\ \phi(\xi, r) = \frac{1}{(\xi^2-r^2)^{\frac{1}{2}}},\ \Delta r = \frac{(r_4-r_1)}{3}.$$

$$\begin{bmatrix}\alpha_1\\ \alpha_2\\ \alpha_3\\ \alpha_4\end{bmatrix} = \tfrac{1}{6}\begin{bmatrix}6 & -11 & 6 & -1\\ 0 & 18 & -15 & 3\\ 0 & -9 & 12 & -3\\ 0 & 2 & -3 & 1\end{bmatrix}\begin{bmatrix}\mu_1\\ \mu_2\\ \mu_3\\ \mu_4\end{bmatrix}$$

$$n_0 = r/\Delta r,\ n_1 = r_1/\Delta r,\ n_4 = r_4/\Delta r.$$

$$\mu_1 = \int_{r_1}^{r_4} \phi(\xi, r)\,d\xi = I_1$$

$$\mu_2 = \frac{1}{\Delta r}\int_{r_1}^{r_4} \phi(\xi, r)(\xi-r_1)\,d\xi = I_2 - n_1 I_1$$

$$\mu_3 = \frac{1}{\Delta r^2}\int_{r_1}^{r_4} \phi(\xi, r)(\xi-r_1)^2\,d\xi = I_3 - 2n_1 I_2 + n_1^2 I_1$$

$$\mu_4 = \frac{1}{\Delta r^3}\int_{r_1}^{r_4} \phi(\xi, r)(\xi-r_1)^3\,d\xi = I_4 - 3n_1 I_3 + 3n_1^2 I_2 - n_1^3 I_1$$

$$I_1 = \ln\left\{\frac{[n_4+(n_4^2-n_0^2)^{\frac{1}{2}}]}{[n_1+(n_1^2-n_0^2)^{\frac{1}{2}}]}\right\}$$

$$I_2 = (n_4^2-n_0^2)^{\frac{1}{2}} - (n_1^2-n_0^2)^{\frac{1}{2}}$$

$$I_3 = \frac{1}{2}\left[n_4(n_4^2-n_0^2)^{\frac{1}{2}} - n_1(n_1^2-n_0^2)^{\frac{1}{2}} + \frac{n_0^2 I_1}{2}\right]$$

$$I_4 = n_4^2(n_4^2-n_0^2)^{\frac{1}{2}} - n_1^2(n_1^2-n_0^2)^{\frac{1}{2}} - \tfrac{2}{3}[(n_4^2-n_0^2)^{\frac{3}{2}} - (n_1^2-n_0^2)^{\frac{3}{2}}]$$

Formula II.

$$\int_{r_1}^{r_4} f(\xi)\phi(r,\xi)\,\mathrm{d}\xi = \alpha_1 f(r_1)+\alpha_2 f(r_1+\Delta r)+\alpha_3 f(r_1+2\Delta r)$$

$$+\alpha_4 f(r_1+3\Delta r), \qquad \phi(r,\xi)=\frac{1}{(r^2-\xi^2)^{\frac{1}{2}}}, \qquad \Delta r=\frac{(r_4-r_1)}{3}$$

$$\begin{bmatrix}\alpha_1\\ \alpha_2\\ \alpha_3\\ \alpha_4\end{bmatrix} = \tfrac{1}{6}\begin{bmatrix}6 & -11 & 6 & -1\\ 0 & 18 & -15 & 3\\ 0 & -9 & 12 & -3\\ 0 & 2 & -3 & 1\end{bmatrix}\begin{bmatrix}\mu_1\\ \mu_2\\ \mu_3\\ \mu_4\end{bmatrix}$$

$$N = r/\Delta r, \qquad n_1 = r_1/\Delta r, \qquad n_4 = r_4/\Delta r.$$

$$\mu_1 = \int_{r_1}^{r_4}\phi(r,\xi)\,\mathrm{d}\xi = I_1$$

$$\mu_2 = \frac{1}{\Delta r}\int_{r_1}^{r_4}\phi(r,\xi)(\xi-r_1)\,\mathrm{d}\xi = I_2-n_1I_1$$

$$\mu_3 = \frac{1}{\Delta r^2}\int_{r_1}^{r_4}\phi(r,\xi)(\xi-r_1)^2\,\mathrm{d}\xi = I_3-2n_1I_2+n_1^2I_1$$

$$\mu_4 = \frac{1}{\Delta r^3}\int_{r_1}^{r_4}\phi(r,\xi)(\xi-r_1)^3\,\mathrm{d}\xi = I_4-3n_1I_3+3n_1^2I_2-n_1^3I_1$$

$$I_1 = \sin^{-1}\left(\frac{n_4}{N}\right)-\sin^{-1}\left(\frac{n_1}{N}\right)$$

$$I_2 = (N^2-n_1^2)^{\frac{1}{2}}-(N^2-n_4)^{\frac{1}{2}}$$

$$I_3 = \tfrac{1}{2}\{[n_1(N^2-n_1^2)^{\frac{1}{2}}-n_4(N^2-n_4^2)^{\frac{1}{2}}]+N^2I_1\}$$

$$I_4 = \tfrac{1}{3}[(n_1^2+2N^2)(N^2-n_1^2)^{\frac{1}{2}}-(n_4^2+2N^2)(N^2-n_4^2)^{\frac{1}{2}}]$$

APPENDIX B

TABLE 1. VALUE OF DYNAMICALLY APPLIED FORCES $P(t)$ NORMALIZED BY THE CORRESPONDING HERTZ FORCE $P_H(t)$, i.e. $P(t)/P_H(t)$

T (μsec) \ a (in.) / t	0·02		0·04		0·06		0·08		0·10		0·12	
	1 μsec	$T/2$	1 μsec	$T/2$	1 μsec	$T/2$	1 μsec	$T/2$	1 μsec	$T/2$	1 μsec	$T/2$
10	1·000	1·000	1·000	1·003	1·000	1·007	0·998	1·012	0·995	1·018	0·991	1·025
40	1·000	1·000	1·000	1·000	1·000	1·000	1·000	1·000	0·999	1·001	0·998	1·002
200	1·000	1·000	1·000	1·000	1·000	1·000	1·000	1·000	1·000	1·000	1·000	1·000

(*Received* 14 *January* 1970; *revised* 5 *August* 1970)

Абстракт—Решая трехмерные уравнения движения, получаются динамические контактные напряжениямежду осесимметрическим снарядом и упругим полупространством. Эти напряжения записываются в виде суммы контактных напряжений Герца и интегралов волнового эффекта. Показано, что в выражениях для радиуса контакта, теория Герца является надлежащим приближением для определения полной приложенной силы. Однако для расчета максимального радиального поверхностного напряжения, при максимальном радиусе контакта, теория Герца применяется только тогда, когда длительность контакта больше чем приблизительно 40 *дсек*. Расхождение между радикльным напряжением Герца и соответствующим значением, полученным в данной работе, оказывается большим в начальном стадии удара, чем в серединном времени контакта.